AGU PUBLICATIONS

JGR

Journal of Geophysical Research: Biogeosciences

RESEARCH ARTICLE
10.1002/2017JG003761

Key Points:
- Elevated surface water and porewater methane concentrations were measured throughout the lagoons despite moderate to marine salinities
- Pollution inputs are likely to substantially enhance methane concentrations and fluxes in mangrove-surrounded lagoon systems
- Ebullition is an important yet under quantified process of methane emissions in the shallow tidally influenced mangrove-lagoon systems

Supporting Information:
- Supporting Information S1

Correspondence to:
A. Paytan,
apaytan@ucsc.edu

Citation:
Chuang, P.-C., M. B. Young, A. W. Dale, L. G. Miller, J. A. Herrera-Silveira, and A. Paytan (2017), Methane fluxes from tropical coastal lagoons surrounded by mangroves, Yucatán, Mexico, *J. Geophys. Res. Biogeosci.*, *122*, 1156-1174, doi:10.1002/2017JG003761.

Received 13 JAN 2017
Accepted 20 APR 2017
Accepted article online 23 APR 2017
Published online 21 MAY 2017

Methane fluxes from tropical coastal lagoons surrounded by mangroves, Yucatán, Mexico

P.-C. Chuang[1,2], M. B. Young[3], A. W. Dale[4], L. G. Miller[3], J. A. Herrera-Silveira[5], and A. Paytan[1,6]

[1]Department of Earth and Planetary Sciences, University of California, Santa Cruz, California, USA, [2]MARUM—Center for Marine Environmental Sciences, University of Bremen, Bremen, Germany, [3]U.S. Geological Survey, National Research Program, Menlo Park, California, USA, [4]Marine Biogeochemie, GEOMAR Helmholtz Centre for Ocean Research Kiel, Kiel, Germany, [5]Departamento de Recursos del Mar, CINVESTAV-IPN Unidad Mérida, Mérida, Quintana Roo, Mexico, [6]Institute of Marine Sciences, University of California, Santa Cruz, California, USA

Abstract Methane concentrations in the water column and emissions to the atmosphere were determined for three tropical coastal lagoons surrounded by mangrove forests on the Yucatán Peninsula, Mexico. Surface water dissolved methane was sampled at different seasons over a period of 2 years in areas representing a wide range of salinities and anthropogenic impacts. The highest surface water methane concentrations (up to 8378 nM) were measured in a polluted canal associated with Terminos Lagoon. In Chelem Lagoon, methane concentrations were typically lower, except in the polluted harbor area (1796 nM). In the relatively pristine Celestún Lagoon, surface water methane concentrations ranged from 41 to 2551 nM. Methane concentrations were negatively correlated with salinity in Celestún, while in Chelem and Terminos high methane concentrations were associated with areas of known pollution inputs, irrespective of salinity. The diffusive methane flux from surface lagoon water to the atmosphere ranged from 0.0023 to 15 mmol CH_4 m^{-2} d^{-1}. Flux chamber measurements revealed that direct methane release as ebullition was up to 3 orders of magnitude greater than measured diffusive flux. Coastal mangrove lagoons may therefore be an important natural source of methane to the atmosphere despite their relatively high salinity. Pollution inputs are likely to substantially enhance this flux. Additional statistically rigorous data collected globally are needed to better consider methane fluxes from mangrove-surrounded coastal areas in response to sea level changes and anthropogenic pollution in order to refine projections of future atmospheric methane budgets.

1. Introduction

Wetlands are the largest natural source of methane (CH_4) to the atmosphere, contributing approximately 20–25% of the total emissions from all anthropogenic and natural sources [*Matthews and Fung*, 1987; *Fung et al.*, 1991; *Whalen*, 2005]. The majority of research on methane emissions from tropical wetlands has been conducted in freshwater systems such as the Amazon Basin [*Bartlett et al.*, 1988, 1990; *Devol et al.*, 1990; *Ringeval et al.*, 2014], and significantly less information is available regarding methane emissions from waterways in coastal saline tropical wetlands and estuaries.

Mangrove ecosystems cover approximately 156,620 km^2 in the tropical and subtropical regions [*Food and Agriculture Organization Forestry*, 2010]. They dominate tropical coastlines worldwide, occurring along shorelines, coastal lagoons, deltas, rivers, creeks, and estuaries. Mangrove forests and the associated water bodies are characterized by high primary productivity, anaerobic sediments, and high soil and sediment organic carbon content [*Gonneea et al.*, 2004; *Kristensen et al.*, 2008a; *Robertson et al.*, 2013; *Ezcurra et al.*, 2016]. Hence, mangrove systems are important sources of organic matter to adjacent estuaries and coastal waters and particularly to the coastal lagoons surrounding them [*Dittmar and Lara*, 2001; *Dittmar et al.*, 2006; *Bouillon et al.*, 2007a, 2008; *Bergamaschi et al.*, 2012, *Maher et al.*, 2013]. In Mexico, mangrove forests cover approximately 7738 km^2 [*Valderrama et al.*, 2014] or one third of Mexico's coastline [*Lankford*, 1977; *Herrera-Silveira and Comín*, 2000]; many of which are surrounded by coastal lagoons.

Data on atmospheric methane fluxes from mangrove-surrounded waterways are sparse, and very little data have been published for these systems in the Americas. *Harriss et al.* [1988] measured an average flux of 0.25 mmol CH_4 m^{-2} d^{-1} from tidally inundated saltwater mangroves in South Florida, while *Barber et al.* [1988] found a much larger flux of 5.1 mmol CH_4 m^{-2} d^{-1} from a low to moderate salinity (1 to 12)

mangrove pond located near Florida Bay. *Sotomayor et al.* [1994] reported methane fluxes between 0.019 and 0.16 mmol CH_4 m^{-2} d^{-1} for unpolluted brackish to marine salinity mangroves in Puerto Rico and fluxes up to 5.1 mmol CH_4 m^{-2} d^{-1} for a similar mangrove area receiving discharge from a sewage treatment plant. This handful of studies constitutes the only reported methane fluxes for water bodies surrounded by mangrove vegetation in the Americas. The lack of information is concerning because the associated water bodies might contribute more methane emissions to the global budgets than the mangrove forests alone. *Duarte et al.* [2005] showed that the area and global contribution of unvegetated coastal sediments to the carbon budget are larger than vegetated habitats (including mangrove forest areas, salt marsh, seagrass, macroalge, and coral reefs). Moreover, unlike mangrove forests, the sediments in the associated mangrove water bodies are continuously submerged, thus enhancing the likelihood for anaerobic conditions and methanogenesis to occur.

More research has been conducted in mangrove-surrounded systems in India. These studies indicate that mangrove-surrounded water bodies can produce methane emissions comparable to those measured in freshwater wetlands [*Purvaja and Ramesh*, 2001; *Purvaja et al.*, 2004; *Verma et al.*, 1999, 2002; *Biswas et al.*, 2004, 2007; *Dutta et al.*, 2015]. The average annual emissions in India range from 0.02 to 11 mmol CH_4 m^{-2} d^{-1} for undisturbed systems and from 7.5 to 59 mmol CH_4 m^{-2} d^{-1} for polluted areas [*Biswas et al.*, 2004, 2007; *Purvaja and Ramesh*, 2001; *Verma et al.*, 1999, 2002; *Dutta et al.*, 2015].

Several characteristics of mangrove-surrounded water bodies, including high organic matter content, high microbial activity, and anaerobic conditions in sediments, may support high rates of methanogenesis even when sulfate is plentiful in the overlying waters [*Bouillon et al.*, 2007b; *Marchand et al.*, 2006; *Chuang et al.*, 2016]. Therefore, a better estimate for the methane flux to the atmosphere from these systems is needed, particularly in developing countries where rapid coastal development is occurring, often with limited pollution control.

We report dissolved methane concentrations in surface water and calculate methane fluxes to the atmosphere at three tropical coastal lagoons in the Yucatán Peninsula, Mexico, where the largest mangrove-lagoon systems of Mexico are located [*Barbier and Strand*, 1998]. The fluxes are compared to methane fluxes from the sediments to the overlying water. In addition, we assess the factors affecting variations in methane concentration and flux and compare polluted and unpolluted areas. This study provides unique and much-needed information about methane emissions from both natural and impacted tropical lagoon systems in the Americas. The results may be representative of other mangrove-surrounded tropical lagoon systems or water bodies and emphasize the need for more through estimation of the global contribution from such settings. A better assessment of methane emissions from mangrove-surrounded water bodies will be useful for evaluating the past and future role of tropical lagoon and estuarine systems to the global methane budget and predicting future inputs from these systems.

2. Study Area

Sampling was conducted in three lagoons with similar vegetation, geology, and climatological patterns, located along the northwest (Gulf of Mexico) coast of the Yucatán Peninsula, Mexico (Figures 1a–1d). The geology of the Yucatán Peninsula is primarily flat-lying Tertiary limestone, and the karstic nature of the region results in very few rivers and little to no surface runoff, except at the height of the rainy season. The typical climatological pattern for the Yucatán Peninsula consists of a dry season from March through May during which rainfall is typically less than 50 mm, a rainy season from June through October during which the majority of the annual rainfall (>500 mm) occurs, and the "nortes" season from November through February, characterized by moderate rainfall (20–60 mm) and intermittent high wind speeds greater than 80 km h^{-1} [*Herrera-Silveira*, 1994]. The average water depth in the lagoons is 120 cm for Celestún Lagoon, 74 cm for Chelem Lagoon [*Chuang et al.*, 2016], and 157 cm for Terminos Lagoon. A wide range of anthropogenic impacts are represented across the three lagoons; Celestún represents relatively natural conditions, Chelem displays moderate anthropogenic impact, and the canals in Terminos Lagoon are highly impacted (see below).

2.1. Celestún Lagoon

Celestún Lagoon (Figure 1b and Table 1) is a relatively undisturbed lagoon located within the Ria Celestún Biosphere Reserve. The port and town of Celestún (population approximately 6000) are located to the

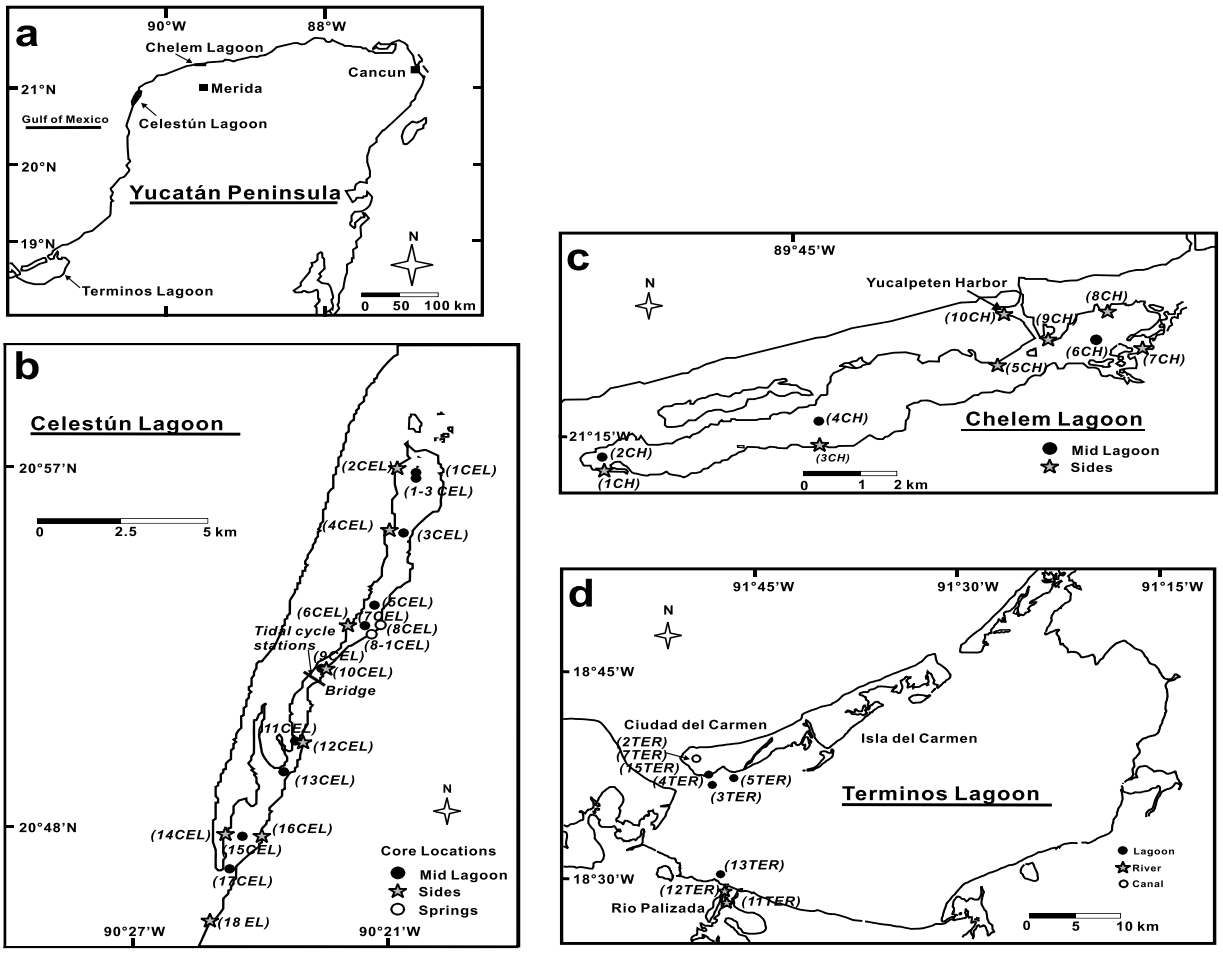

Figure 1. Maps of (a) the Yucatán Peninsula with lagoon locations, (b) Celestún Lagoon, (c) Chelem Lagoon, and (d) Terminos Lagoon. Individual sampling stations are marked, except for the canal stations in Terminos Lagoon, which are grouped for clarity.

west of the lagoon, and at the time of this study there was no significant urban or industrial development near the shores of the lagoon. The lagoon is long and narrow and generally very shallow (average depth 120 cm) except for a narrow boat channel (depth ~ 2 m) that extends approximately two thirds of the length of the lagoon. The water in the lagoon has a relatively short residence time due to tidal exchange, and it is well mixed and oxygenated. Brackish groundwater discharges into Celestún from large springs located in the northern and middle parts of the lagoon, and from many small springs throughout the lagoon [*Herrera-Silveira*, 1994; *Young et al.*, 2008] resulting in a year-round salinity gradient. Long-term nutrient monitoring in Celestún shows no evidence of eutrophication or significant pollution inputs.

Table 1. Comparison of Lagoon Characteristics

	Celestún[a]	Chelem[a]	Terminos
Surface area (km^2)	28	13.6	1800[b]
Volume (m^3)	33×10^6	16.3×10^6	8750×10^{6}[c]
Average depth (m)	1.2	0.74	1.57[d]
Salinity range	5–37	25–48	0–39[e]
Tidal type, range (m)	Mixed diurnal, 0.5[d]	Diurnal, 0.6[f]	Mixed diurnal, 0.3[b]

[a] *Herrera-Silveira et al.* [1998].
[b] *Rivera-Monroy et al.* [1998].
[c] *Eagle* [2002].
[d] This study.
[e] *Day et al.* [1982].
[f] *Valdes and Real* [1998].

Celestún is surrounded by approximately 22.3 km^2 of well-developed mangrove forest consisting of *Avicennia germinans*, *Rhizophora mangle*, and *Laguncularia racemosa*. Extensive algae and seagrass beds are present throughout the lagoon, covering approximately 65% of the lagoon sediment [*Gonneea et al.*, 2004; *Herrera-Silveira et al.*, 1998].

2.2. Chelem Lagoon

Chelem Lagoon (Figure 1c and Table 1) is located near the port city of Progreso (population 45,000) and has been significantly impacted by urban and industrial developments [*Valdes and Real*, 1998; *Herrera-Silveira et al.*, 2000; *Tapia González et al.*, 2008]. The hydrological characteristics of the lagoon underwent significant change in 1969 when the construction of Yucalpeten Harbor created a large channel to the sea near the middle of the lagoon [*Valdes and Real*, 1998]. Evidence of altered nutrient levels consistent with eutrophication due to human activities have been observed in Yucalpeten Harbor and the eastern section of this lagoon [*Valdes and Real*, 1998; *Herrera-Silveira et al.*, 2000; *Tapia González et al.*, 2008], while it appears that the western section has not experienced large anthropogenic impacts [*Valdes and Real*, 1998; *Herrera-Silveira et al.*, 2000]. Chelem has high evaporation rates and receives very little groundwater discharge, resulting in relatively high salinities, which ranged from 24.8 in the western lagoon to 40.3 in the eastern lagoon, during this study. The lagoon is shallow (74 cm), and the water column is mixed and well oxygenated. Vegetation in and around Chelem Lagoon consists of a scrub mangrove forest dominated by *A. germinans* and *R. mangle* that surrounds most of the lagoon, along with algae and seagrasses that cover less than 30% of the lagoon sediment [*Herrera-Silveira et al.*, 1998].

2.3. Terminos Lagoon

Terminos Lagoon (Figure 1d and Table 1), one of the largest estuary in Mexico (1800 km^2), is located at the southwestern edge of the Yucatán Peninsula. The lagoon is wide and shallow (average depth 157 cm) and has two open connections to the Gulf of Mexico that are located on either side of the barrier island of Isla del Carmen. The city of Ciudad del Carmen (population 130,000) is located on this barrier island, and there are significant inputs of wastewater and other pollution to the mangrove forest and canals located near the city [*Gonneea et al.*, 2004]. Terminos is the only one of the three lagoons that receives river discharge, and salinities within the lagoon area range from 0 at the river mouths to coastal seawater salinities (35 to 39) throughout most of the lagoon and the city canals. Overall, Terminos is a well-oxygenated environment with average dissolved oxygen concentrations of >4.7 mg L^{-1} that did not show strong seasonal differences or differences between fluvial subsystems within the lagoon [*Medina-Gómez et al.*, 2015]. The shorelines of Terminos Lagoon are covered with fringe mangrove forests dominated by *R. mangle*, *A. germinans*, and *L. racemosa* that experience regular tidal inundation [*Day et al.*, 1996]. Extensive basin mangrove forests, also dominated by the same mangrove species, are present beyond the fringe mangrove forests on the mainland shores of Terminos Lagoon, but rarely experience tidal inundation. Seagrass beds cover a very small portion of the lagoon sediment [*Yanez-Arancibia and Day*, 1982; *Day et al.*, 1996].

3. Sampling Methods

3.1. Sampling Strategy and Timing

In order to estimate an average atmospheric methane flux from the Yucatán lagoons as accurately and practically as possible, samples were collected at various locations within the lagoons over both short (hours) and longer (years) time scales. Celestún was the focus of intensive sampling efforts due to its relatively undisturbed condition that may best represent the natural preanthropogenic methane flux from the Yucatán tropical lagoon systems. To capture the short-term (e.g., tidal and diurnal) variability in methane concentrations, we collected samples during different stages of a tidal cycle at three representative stations in Celestún Lagoon.

Seasonal variations in methane concentrations and fluxes were addressed by conducting four sampling trips over the course of 2 years. The sampling trips were chosen to coincide with each of the three seasons of the Yucatán Peninsula: April 2000 (dry season), December 2000 (nortes season), October 2001 (late rainy season), and July 2002 (early rainy season). Most of the work was conducted at Celestún Lagoon, which has significant groundwater input and a permanent salinity gradient, and at Chelem Lagoon that has little to no groundwater input, marine to hypersaline salinities, and localized pollution within the harbor. In

both lagoons, samples were collected along lengthwise transects and from the sides and middle of the lagoons. In addition, samples were collected from several springs in Celestún and from the harbor area in Chelem. During the October 2001 sampling, samples were also collected in Terminos Lagoon in order to examine a range of anthropogenic impacts within a single lagoon including relatively natural conditions, localized moderate impacts, and areas with large amounts of direct wastewater discharge. Specifically, samples were collected from three distinct areas within Terminos: (1) Rio Palizada, a river entering the south part of the lagoon (salinity = 0.6 ± 0.3), (2) the main lagoon, with samples taken from the center and sides (salinity = 20.7 ± 11.9), and (3) a polluted seawater canal running from the lagoon mouth through Ciudad del Carmen (salinity = 23.3 ± 5.9). Various direct pollution inputs were observed during sample collection, including street runoff, waste from outhouses located on the banks of the canals (less than 1 m from the high tide line), and washing of boats and laundry within the canals. Samples collected from Celestún Lagoon, Chelem Lagoon, and Terminos Lagoon are denoted by CEL, CH, and TER, respectively.

3.2. Collection of Surface Water and Porewater Samples for Methane Concentration Analysis

Surface water samples were collected by direct filling of sample containers from the upper 10 cm of the water column. Spring samples (site 8CEL) were collected using a Niskin bottle and immediately transferred into sample containers. In April 2000, December 2000, and October 2001, samples were transported off site for methane analysis. Duplicate (April 2000 and December 2000) or triplicate (October 2001 and July 2002) samples were collected at all stations.

Sediment cores were collected along lengthwise transects in both lagoons during the three different seasons. Sampling was conducted in Celestún and Chelem in April 2000 (dry season), December 2000 (nortes season), and October 2001 (late rainy season). Additional sampling was conducted in Celestún during July 2002 (early rainy season). Two cores were collected at most stations along the transects; one from the side of the lagoon and one from the center, in order to investigate differences related to proximity to mangrove vegetation. Subsamples for porewater methane concentration analysis were collected as described in *Chuang et al.* [2016].

4. Analytical Methods

4.1. Methane Concentration Analyses

Methane concentrations for all samples were measured on a SRI 310 gas chromatograph equipped with a flame ionization detector and an Alltech Haysep S 100/120 column (1.8 m × 0.3 cm × 0.2 cm). Helium was used as the carrier gas at a flow rate of 15 mL/min, and the column and detector temperatures were maintained at 50°C and 150°C, respectively. Peak integration was performed using Peak Simple NT software. Methane gas standards were prepared by diluting 100% methane in helium, and five standards, bracketing the range of sample concentrations, were measured at the beginning, middle, and end of each set of analyses. Average standard error of repeat injections of standards throughout a sample run (between 2 to 6 h of continuous analysis) was 1.8% (n = 152). Porewater methane concentrations were measured as described in *Chuang et al.* [2016].

4.1.1. Dissolved Methane Concentrations

Dissolved methane concentrations in water samples were measured using a headspace equilibration technique modified from *Rudd et al.* [1974]. During April 2000, December 2000, and October 2001, samples were collected in 125 mL glass serum bottles, sealed without headspace using blue butyl stoppers, and saturated $HgCl_2$ solution (0.3 mL) was added immediately after sample collection to halt all biological activity. Headspace equilibration was performed in the laboratory just prior to analysis. For headspace equilibration, 40 mL of sample water was drawn into a 60 mL plastic syringe, and equilibrated with 20 mL of ambient air by vigorous shaking for 2 min, followed by standing equilibration for 3 min. During the July 2002 trip, a gas chromatograph was transported to the sampling site, surface water samples were collected directly into 60 mL syringes, and headspace equilibration was performed at each sampling station. The headspace gas was then injected into either a 10 mL Mark-M tube prefilled with degassed Milli-Q water and sealed with a black butyl stopper or a 10 mL preevacuated Exetainer. All gas samples were analyzed within 10 h of transfer to the Mark-M tube or Exetainer.

The dissolved methane in the surface water samples (C_w) was calculated by adding the measured headspace methane concentration and the amount of methane remaining in the water sample after headspace equilibration, calculated from the solubility equation of *Yamamoto et al.* [1976] (the atmospheric methane contribution was accounted for but was always negligible). The average combined standard error of sampling, transport, and analysis (determined from triplicate samples) was 9.3% (n = 60 sets of triplicate samples), for the April 2000, December 2000, and October 2001 campaigns, and 4.8% (n = 23 sets) for July 2002 which did not require extended sample transport because the gas chromatograph was brought to the field site.

4.2. Methane Flux Estimates Using Floating Chambers

Floating flux chambers were deployed at four stations in Celestún, two stations in Chelem, and six stations in Terminos during October 2001 (Table S1 in the supporting information). Each chamber consisted of a 27.6 × 27.6 × 7.0 cm clear acrylic top sealed to a 27.9 × 27.9 × 19.0 cm aluminum base (chamber volume = 20.1 L) surrounded by closed-cell foam for floatation. The acrylic top was fitted with a sampling port consisting of a Swagelok tubing connector, a 10 cm length of tygon tubing, and a three-way stopcock, which allowed for headspace sampling to be conducted from a small boat. Headspace samples were collected every 10 min for between 30 and 40 min, starting immediately after the chamber's top was installed. Ambient air samples were collected outside of each chamber at the time of placement to ensure that methane concentrations within the chamber at the start of the sampling period were not different than ambient air concentrations as a result of chamber placement in the water. Chamber headspace samples were collected using a 10 mL Glaspak syringe and were immediately transferred to butyl-stoppered glass serum bottles by displacing a volume of de-gassed water. The de-gassed water was prepared by sparging with helium for at least 15 min, after which time no methane was detectable in the de-gassed water.

4.3. Environmental Parameters

Dissolved oxygen, temperature, and salinity were measured at each station using a YSI model 85 probe. Air temperature was measured using a factory-calibrated thermistor. Minimum, maximum, and average wind speeds at each station were measured using a handheld anemometer positioned 1 m above the lagoon surface. Water depth and vegetation type were recorded at each station. A Vector acoustic Doppler velocimeter and an Ocean Sensors OS2000 CTD (conductivity, temperature, and depth) were deployed in order to measure water depth, current velocities, temperature, and salinity during the sampling period from 13 to 17 July 2002. The instruments were deployed together in the boat channel directly in front of the Ducks Unlimited de Mexico (DUMAC) field station near the midpoint of the lagoon approximately 420 m north of the Celestún bridge (Figure 1).

Meteorological data such as wind speeds for Celestún were obtained from the DUMAC weather station, which provided meteorological information in 10 min intervals. Meteorological data for Chelem and Terminos were obtained through the NOAA Surface Data database, which provided daily averages from the Progreso Station (near Chelem) and the Ciudad del Carmen Station (near Terminos).

5. Methane Flux Calculations

5.1. Diffusive Fluxes From the Surface Water to the Atmosphere

Diffusive methane fluxes from the lagoon water to the atmosphere were calculated from surface water dissolved methane concentrations using the gas-transfer model of *Wanninkhof* [1992] and the general stagnant film equation [*Liss and Slater*, 1974]:

$$J = k_v \cdot (C_w - C_{eq}) \quad (1)$$

where J is flux of gas to the atmosphere (in mmol m^{-2} d^{-1}), k_v is gas transfer velocity (in m d^{-1}), C_w is measured concentration of dissolved methane in water (in mmol m^{-3}), and C_{eq} is concentration of methane in equilibrium with the atmosphere at in situ temperature (in mmol m^{-3}). C_{eq} was calculated for each sample from the temperature- and salinity-dependent equilibrium relationship of *Wiesenburg and Guinasso* [1979]. The k_v was calculated using the relationship between gas transfer and wind speed developed by *Wanninkhof* [1992]:

$$k_v = 0.31 \cdot u^2 \cdot \left(\frac{Sc}{660}\right)^{-\frac{1}{2}} \quad (2)$$

where k_v has units of cm h^{-1}, u is wind speed at 10 m height (in m s^{-1}), and Sc is the Schmidt number for methane calculated for in situ temperature and salinity using the experimentally determined diffusion coefficients from *Jähne et al.* [1987]. Wind speed measurements from the sampling stations were scaled to 10 m height using the equation from *Liss and Merlivat* [1986]:

$$u_{z=10\mathrm{m}} = 1.29 u_{z=1\mathrm{m}} \quad (3)$$

where $u_{z=10\mathrm{m}}$ is the wind speed at 10 m (in m s^{-1}) and $u_{z=1\mathrm{m}}$ is the wind speed at 1 m (in m s^{-1}).

The average diffusive methane flux from the water to the atmosphere for each lagoon during a particular trip was estimated by calculating the average methane flux for each lagoon zone (determined by using average methane concentration, temperature, and salinity from all stations within that zone) and the relative surface area of each zone. Celestún was divided into an inner, middle, and outer zone based on salinity distribution and lagoon shape, and Chelem was divided into a lagoon zone and a harbor zone. Stations in Terminos were divided into river (Rio Palizada), lagoon, and city canal groups. Since diffusive flux calculations are highly sensitive to wind speed, we chose also to use the average seasonal wind speeds (from the weather station at each lagoon) in order to better estimate the range of fluxes over longer time periods. It is important to note that no significant differences were found between fluxes calculated using our direct measurements of wind speed and air temperature throughout the lagoons and those recorded by the weather stations near each lagoon (Table S1).

5.2. Total Fluxes From the Surface Water to the Atmosphere

The chambers capture the total flux to the atmosphere including both flux by diffusion and by ebullition (bubble flux), although the diffusive flux is likely to be under estimated due to zero wind impact inside the chambers. Initial methane concentrations within the chambers were all identical, within analytical error, to ambient air methane concentrations.

Since flux chambers collect methane released by both diffusion and ebullition, a least squares linear regression was applied to determine which type of flux was dominant for each chamber deployment [*Miller and Oremland*, 1988]. Specifically, it was expected that diffusive fluxes would show a linear increase in methane concentration in the chamber over time while ebullition would result in sporadic pulses (large spikes) of methane. Chambers generally showed distinct nonlinear increases in methane concentration, which in several instances coincided with direct observation of ebullition and final headspace concentrations well above equilibrium with the surface water. The total flux was thus determined from the difference between initial and final headspace methane concentrations in the flux chambers.

5.3. Benthic Methane Fluxes and Methanogenesis Rates

A numerical transport-reaction model was used to simulate the measured down-core dissolved methane concentrations in order to estimate total sediment to water column flux and methane production by microbial methanogenesis [*Chuang et al.*, 2016; see simulations for different profile types therein]. The net rate of methane production and transport of dissolved methane in the upper 20 cm of the sediments was quantified by applying the following equation at steady state [*Berner*, 1980; *Boudreau*, 1997]:

$$\Phi \cdot \frac{\partial C}{\partial t} = \frac{\partial\left(\Phi \cdot Ds \cdot \frac{\partial C}{\partial x}\right)}{\partial x} - \frac{\partial(\Phi \cdot v \cdot C)}{\partial x} + \Phi \cdot R_{\mathrm{CH_4}} \quad (4)$$

where x (cm) is sediment depth, t (yr) is time, Φ (dimensionless) is porosity, Ds (cm^2 yr^{-1}) is the solute-specific diffusion coefficient in the sediment, C (mmol cm^{-3}) is the concentration of methane in the porewater, and v (cm yr^{-1}) is the burial velocity of porewater. This latter term was found to make a negligible contribution to the methane flux and is included here for consistency [*Chuang et al.*, 2016].

$R_{\mathrm{CH_4}}$ (mmol cm^{-3} yr^{-1}) in equation (4) is the net methane production rate and is proportional to the difference between modeled ($C_{\mathrm{CH_4}}$) and measured concentrations ($C_{\mathrm{CH4_{OBS}}}$).

$$R_{CH_4} = k_{CH_4} \cdot (C_{CH4_{OBS}} - C_{CH_4}) \quad (5)$$

where k_{CH_4} is the corresponding kinetic constant, 100 to 1000 year^{-1} [*Chuang et al.*, 2016] (Table S2).

Methane fluxes (mmol cm^{-2} yr^{-1}) at the model boundaries were calculated as follows:

$$F_{CH_4}(x) = \Phi(x) \cdot \left(v(x) \cdot C_{CH_4} - Ds \cdot \frac{dC_{CH_4}(x)}{dx} \right) \quad (6)$$

where x = 20 cm is the bottom of the simulated core and x = 0 cm is the sediment-water interface. In this study, positive fluxes are directed out of the sediment to the water column (most of model-derived fluxes were positive; Table S2).

Parameterization of the equations above has been described in detail by *Chuang et al.* [2016] (see also Tables S1 and S2). Equation (4) does not take into account transport of methane out of the sediment by ebullition [*Chuang et al.*, 2016]. Consequently, the net rate of methane production and the total methane flux at the sediment-water interface will be underestimated for the sediments where methane porewaters are supersaturated.

6. Results

6.1. Surface Water Methane Concentrations and Seasonal Variations

Surface water dissolved methane concentrations within the three lagoons during the full sampling period ranged from 25 nM (Chelem) up to 8378 nM (Terminos) (Figure 2 and Tables S1a–S1c). The average methane concentrations in the polluted canals connected to Terminos were the highest (3505 ± 3436 nM) of any zone within the three lagoons. The second highest average concentrations were found in the inner zone of Celestún during all seasons, and the lowest average concentrations were found in the main lagoon part of Chelem and the outer zone of Celestún. Overall dissolved methane concentrations at Chelem and Terminos Lagoons are typically less than 300 nM, but some polluted stations had much higher concentrations contributing to the high variability in the reported concentrations (Tables S1b and S1c).

In Celestún, measured methane concentrations ranged from 41 nM to 2551 nM, with the highest concentrations in the inner zone of the lagoon (average salinity = 17.7) and the lowest concentrations in the outer zone toward the lagoon mouth (seawater salinity) (Figure 2a). Average water depths at the sampling stations were not different between the different lagoon zones, indicating that the higher methane concentrations were not the result of depth-related dilution effects (Table S1a). The highest average air and water temperatures in Celestún were measured during the rainy season (October 2001 and July 2002), while the highest average wind speeds were measured during the dry season (April 2000) (Table S1a). The average water and air temperatures were significantly lower during the nortes season (December 2000) than at any other sampling time (Table S1a). No significant differences in water temperature, air temperature, or wind speed between the lagoon zones were detected at any given season, suggesting that these parameters were not responsible for the spatial variability in surface water methane concentrations throughout the lagoon at any given season (Figure 2 and Table S1a). Water inputs to Celestún Lagoon are seawater and groundwater from submarine springs, and both have lower methane concentrations than those observed in the lagoon water, indicating an internal source of methane, most likely a sedimentary methane flux [*Chuang et al.*, 2016].

In Chelem, surface water methane concentrations ranged from 25 nM to 1796 nM (Figure 2c). In contrast to Celestún, surface water methane concentrations in Chelem did not show any distinct salinity-related spatial patterns within the main lagoon. The east side of the lagoon had slightly higher average salinities than the west side of the lagoon during all trips, but methane concentrations were similar. Two sites, one at the far west side of Chelem (1CH) and the other within the harbor area (10CH), showed substantially elevated surface water methane concentrations in comparison to other stations during one or more of the sampling trips. The elevated methane concentrations at both sites appeared to be highly localized and not associated with differences in salinity, water temperature, or water depth. No significant differences were observed in the average methane concentrations within Chelem between the three different sampling trips. However, the lowest average methane concentrations did coincide with higher average salinity which occurred during the April 2000 (dry season) trip (Figures 2c–2d) probably due to mixing with seawater that had lower methane concentrations.

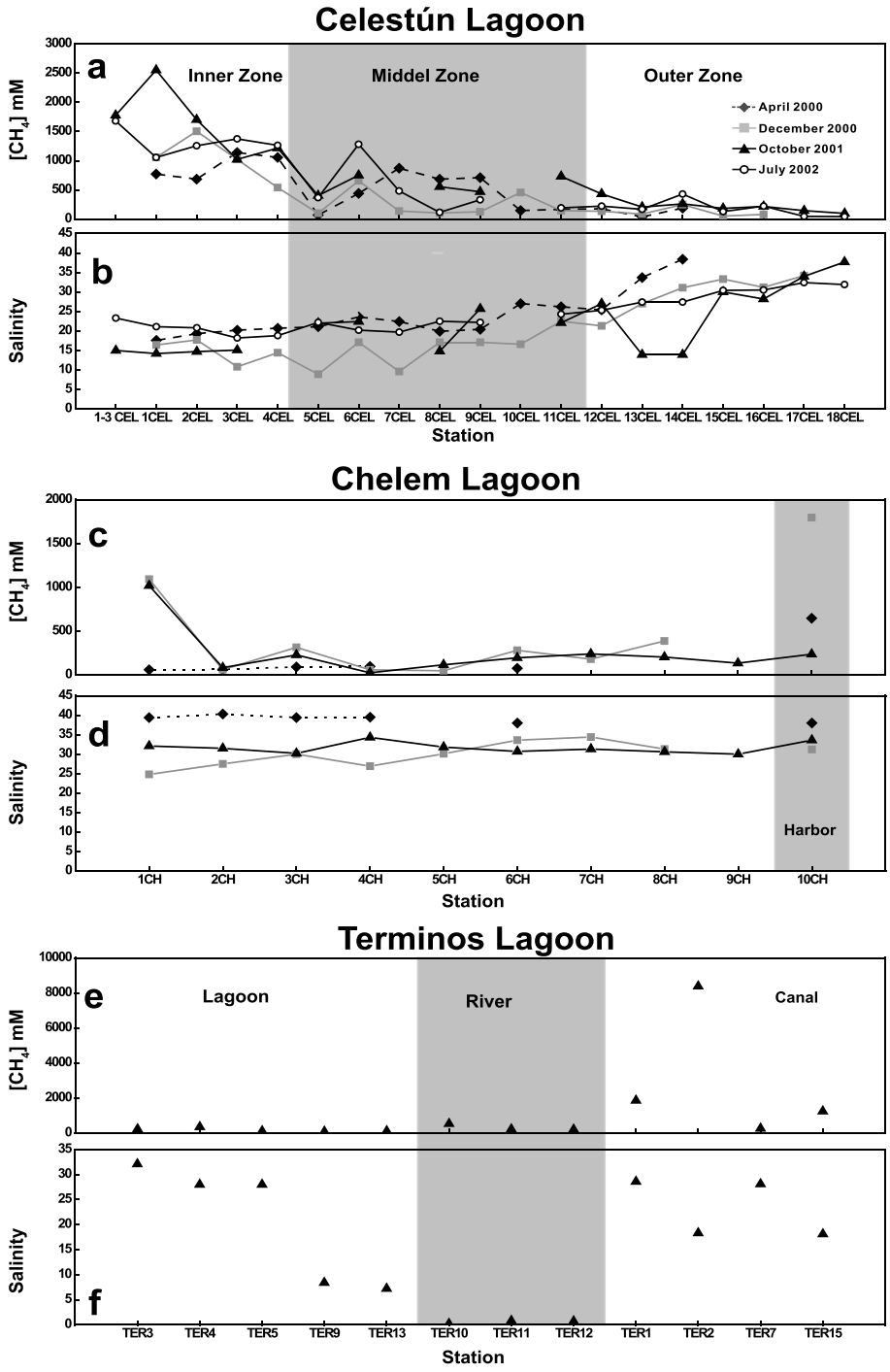

Figure 2. Surface water methane concentrations (a, c, e) and salinity (b, d, f) in Celestún, Chelem, and Terminos Lagoon. Stations classified as middle zone, harbor and river for the three lagoons are in shaded grey.

Surface water methane concentrations in Terminos show very high variability and ranged from 85 nM to 8378 nM, with the highest concentrations occurring in a polluted canal (Figure 2e). The average methane concentrations in the lagoon and river stations were 180 ± 110 nM and 320 ± 186 nM, respectively. The methane concentrations in the city canal samples were highly variable, ranging from 261 nM to 8378 nM, with an average of 3505 nM. The average methane concentration in the canal samples was significantly different from that of the river and the lagoon samples. Interestingly, the river water samples, which had very low salinities (<1), had a similar range of surface water methane concentrations as the lagoon samples,

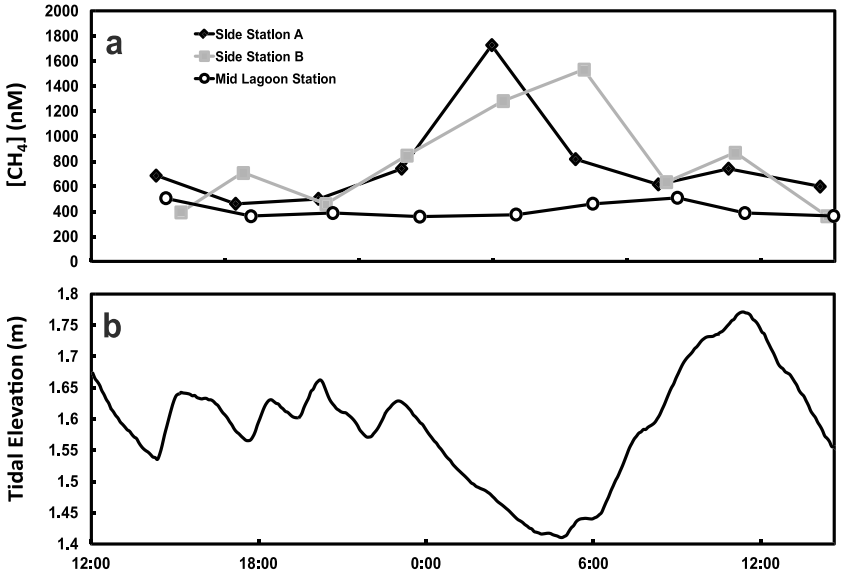

Figure 3. Variations of (a) surface water methane concentrations over 24 h from 16 to 17 July 2002 at two stations near the side of the lagoon (side stations A and B; water depth $<$ 1 m) and one station near the center of the lagoon (midlagoon station; water depth ~ 1.75 m). (b) Tidal height was obtained from the CTD deployed in close proximity to these three stations.

despite the higher salinities in the lagoon itself (salinity range 7 to 32). Only one excursion was made to Terminos; hence, there are no seasonal data for this lagoon. In both Chelem and Terminos, areas with direct pollution inputs had much higher methane concentrations than areas farther away from pollution sources.

6.2. Surface Water Methane Concentrations and Tidal Variations

The tidal height in Celestún varied little over the first 12 h of observations and then showed a clear increase and decrease of $>$40 cm over the subsequent hours. This unusual behavior is probably caused by the effect of a mixed semidiurnal tide combined with lagoon geometry, bathymetry, and friction [*Kjerfve*, 1981; *Tenorio-Fernandez et al.*, 2016]. Tidal variations in surface water methane concentrations showed much greater variability at the sides of the lagoon in comparison to the mid lagoon (Figure 3). Concentrations varied by approximately 50% over the course of a tidal cycle at the shallow stations at the side of the lagoon, while the variations in the midlagoon station were only ~15%.

6.3. Methane Fluxes at the Water-Air Interface and Flux Chamber Measurements

The diffusive methane fluxes from the lagoon water to the air, calculated per unit area at the water-air interface, are presented in Figure 4 and Table S1. The fluxes ranged from 0.0023 to 15 mmol CH_4 m^{-2} d^{-1}. The highest values are up to 2 orders of magnitude higher than previously reported fluxes from other mangrove-surrounded waters calculated by the gas-transfer model, e.g., Andaman Island (0.11 to 0.47 mmol CH_4 m^{-2} d^{-1} [*Linto et al.*, 2014]), India (0.002 to 0.134 mmol CH_4 m^{-2} d^{-1} [*Biswas et al.*, 2007]), Tanzania (0.07 to 0.35 mmol CH_4 m^{-2} d^{-1} [*Kristensen et al.*, 2008b]), and Australia (0.01 to 0.63 mmol CH_4 m^{-2} d^{-1} [*Call et al.*, 2015]). In Celestún Lagoon, as expected from the distribution of methane concentrations in the surface waters, the highest diffusive methane fluxes were in the inner zone and the lowest fluxes were measured in the outer zone (Figure 4a). This trend is consistent for all seasons (Tables 2 and S1a). At Chelem, higher methane fluxes were recorded at the far west side and in the pollution-impacted harbor area (Figure 4b and Tables 2 and S1b). The highest diffusive methane flux was calculated at one of the canal sites in Terminos where the flux was over 10 times higher than in the river and the lagoon (Figure 4b and Table S1c).

Gas bubbles were observed regularly in the lagoons during all seasons particularly at low tide. Although the number of chambers deployed was too small to capture the variability in ebullition of methane from the lagoons [*Keller and Stallard*, 1994; *Bastviken et al.*, 2004; *Podgrajsek et al.*, 2014], our objective was to

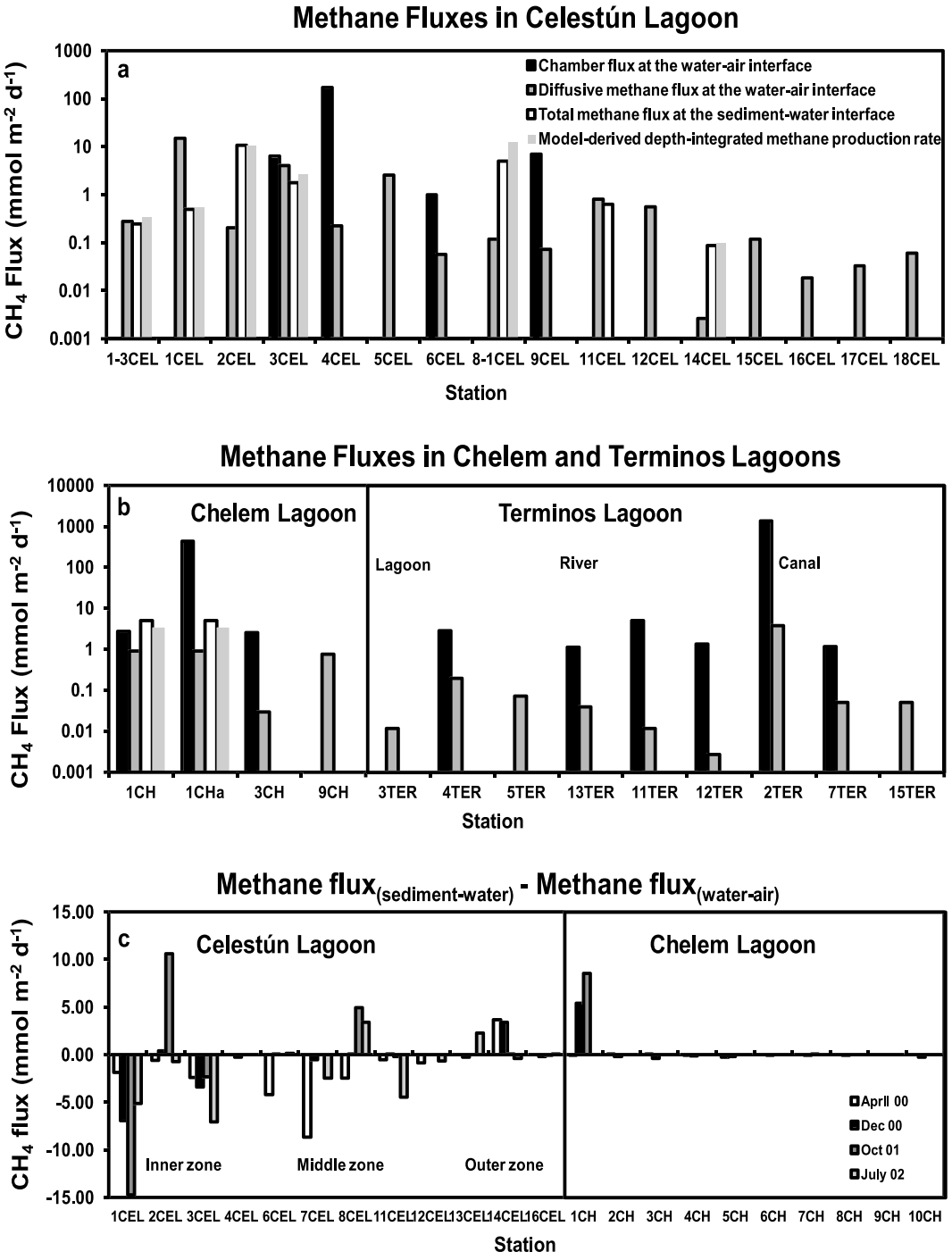

Figure 4. Comparison of calculated diffusive methane flux at the water-air interface, total methane flux at the sediment-water interface, depth-integrated methane production rate, and measured chamber flux: (a) Celestún and (b) Chelem and Terminos Lagoons during October 2001. Methane concentrations are log scale. Two chambers were used at station 1CH: chamber 1CH was deployed in deeper water (30 cm) compared to 1CHa (~10 cm). (c) Modeled total methane flux at the sediment-water interface (equation (6)) minus the calculated flux at the water-air interface (equation (1)) in Celestún and Chelem Lagoons during four sampling trips. Please note that in Figures 4a and 4b , sediment cores were not taken at all stations.

determine whether the total methane flux is higher than the calculated diffusive flux. Indeed, chamber fluxes (mean = 46.5, 144, and 233 mmol CH_4 m^{-2} d^{-1} for Celestún, Chelem, and Terminos Lagoons, respectively) are consistent with ebullition being between 1.5 and 760 times greater than the calculated diffusive fluxes

Table 2. Average Diffusive Methane Flux Across the Water Surface Calculated for Celestún, Chelem, and Terminos Lagoons[a]

Lagoon, Season, and Zone	CH_4 Flux (mmol CH_4 m^{-2} d^{-1})	Total Area (km^2)	Total CH_4 Flux (g CH_4 yr^{-1})
Celestún: April 2000 (Seasonal Wind Speed = 6.8 ± 2.4 m s^{-1})			
Inner	3.8	9.36	$2{,}050 \times 10^3$
Middle	2.8	7.99	$1{,}280 \times 10^3$
Outer	0.56	9.31	300×10^3
All[b]	2.3	26.66	$3{,}630 \times 10^3$
Celestún: Dec 2000 (Seasonal Wind Speed = 5.6 ± 2.3 m s^{-1})			
Inner	2.5	9.36	$1{,}360 \times 10^3$
Middle	0.63	7.99	290×10^3
Outer	0.23	9.31	130×10^3
All[b]	1.1	26.66	$1{,}780 \times 10^3$
Celestún: Oct 2001 (Seasonal Wind Speed = 5.5 ± 2.2 m s^{-1})			
Inner	4.5	9.36	$2{,}100 \times 10^3$
Middle	1.8	7.99	640×10^3
Outer	0.75	9.31	310×10^3
All[b]	2.0	26.66	$3{,}050 \times 10^3$
Celestún: July 2002 (Seasonal Wind Speed = 5.5 ± 2.2 m s^{-1})			
Inner	3.8	9.36	$2{,}100 \times 10^3$
Middle	2.3	7.99	$1{,}080 \times 10^3$
Outer	0.62	9.31	340×10^3
All[b]	2.3	26.66	$3{,}520 \times 10^3$
Chelem: Apr 2000 (Seasonal Wind Speed = 3.0 ± 0.9 m s^{-1})			
Lagoon	0.061	13.6	48×10^3
Harbor	0.294	0.6	10×10^3
All[b]	0.069	14.0	58×10^3
Chelem: Dec 2000 (Seasonal Wind Speed = 2.5 ± 1.0 m s^{-1})			
Lagoon	0.16	13.6	110×10^3
Harbor	0.88	0.6	60×10^3
All[b]	0.21	14.0	170×10^3
Chelem: Oct 2001 (Seasonal Wind Speed = 2.3 ± 0.7 m s^{-1})			
Lagoon	0.12	13.6	100×10^3
Harbor	0.16	0.6	4.1×10^3
All[b]	0.13	14.0	104×10^3
Terminos: Oct 2001 (Seasonal Wind Speed = 4.9 ± 1.2 m s^{-1})			
Lagoon	0.38	1,800	$40{,}100 \times 10^3$
River	0.66	?	
Canals	7.7	2	900×10^3
All[c]	0.39	1,802	$41{,}000 \times 10^3$

[a]Wind speeds are reported as seasonal averages and standard deviation collected by weather stations at 10 m height.
[b]Methane flux reported as an area-weighted average for each lagoon and season.
[c]Fluvial methane flux and area not included in calculation. The polluted sites were also not included in the averages calculated due to their large variability.

(Figure 4 and Tables S1a and S1b). Chamber fluxes did not correlate with surface water methane concentrations or with any other measured environmental parameter, suggesting sporadic bubble release from the sediments [see *Chuang et al.*, 2016].

6.4. Porewater Methane Concentrations and Fluxes to the Water Column

Methane concentrations in porewater and fluxes from sediment cores collected at both Chelem and Celestún are shown in Figures 4 and S1 and Table S1 [see also *Chuang et al.*, 2016]. Porewater methane profiles in these cores collectively show different trends such as a single distinct peak within the upper 5–20 cm (e.g., 1CEL_Jul02), multiple small peaks (e.g., 8CEL_Oct01), a gradual increase of concentration with sediment depth (e.g., 1CEL_Apr00), or no change with depth (e.g., 2CH_Dec00 and 7CH_Oct01). Large variability in both the concentration of porewater methane and shape of the concentration profile was seen throughout both lagoons, and the distribution of profile types was not spatially or temporally systematic. Based on *Chuang et al.* [2016], the source of methane to lagoon waters is from production within the sediment and transport to the water column mainly by diffusion and gas bubble release.

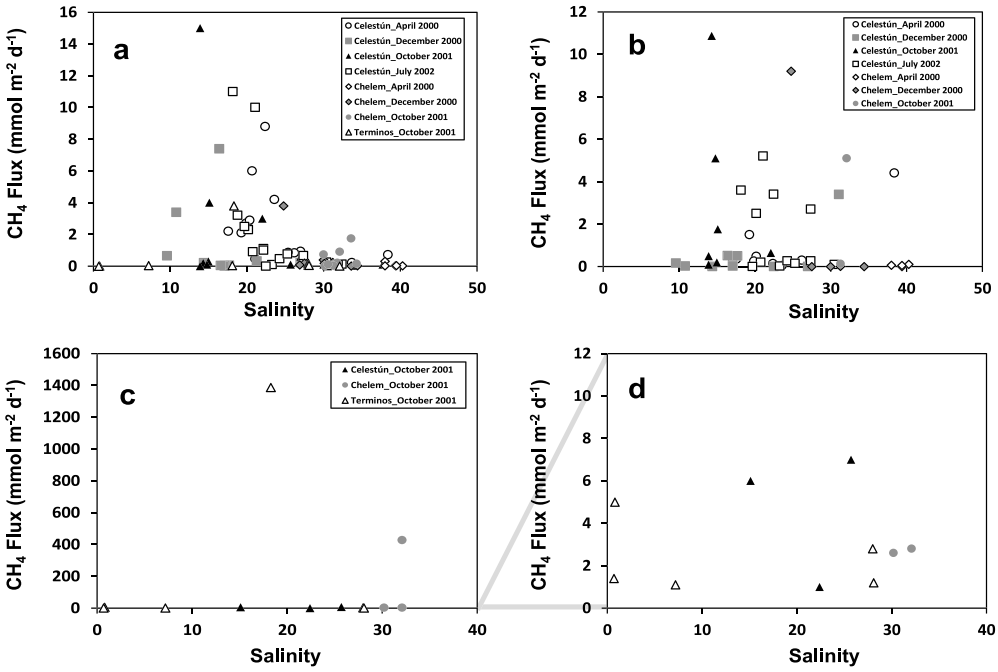

Figure 5. Relationship between (a) diffusive methane flux at the water-air interface and salinity, (b) total methane flux at the sediment-water interface and salinity, and (c) chamber flux at the water-air interface and salinity. Figure 5d shows an enlarged version of Figure 5c at low methane flux.

7. Discussion

7.1. Elevated Methane Concentrations in Surface Waters and Porewaters

Previous studies in moderate to high-salinity wetlands and water bodies (other than mangrove-surrounded systems) typically show much lower surface water methane concentrations and atmospheric methane emissions than in freshwater wetlands [*Bartlett et al.*, 1985, 1987; *Rejmankova and Post*, 1996; *Segarra et al.*, 2013]. Presumably, this is in part due to high concentrations of sulfate in seawater favoring sulfate reduction and anaerobic methane oxidation (AOM) [*Barnes and Goldberg*, 1976]. An inverse log linear relationship between salinity and methane emissions has been shown for data compiled from 31 tidal marshes [*Poffenbarger et al.*, 2011]. However, the methane distribution and flux results from the three lagoons of the Yucatán Peninsula strongly suggest that salinity is not the primary controlling factor (e.g., limiting) for methane flux from mangrove-dominated ecosystems. Surface water and porewater methane concentrations were not correlated with salinity as seen in Figure 2 and reported in *Chuang et al.* [2016]. Consequently, there are poor or no clear relationships between salinity and methane fluxes. For example, $r^2 = 0.090$ ($r = 0.30$; $p < 0.003$) is calculated for the relationship between the diffusive methane flux at the water-air interface and salinity (Figure 5a), $r^2 = 0.001$ ($r = 0.03$; $p > 0.05$) for the relation between total methane flux at the sediment-water interface and salinity (Figure 5b), and $r^2 = 0.003$ ($r = 0.05$; $p > 0.05$) for chamber flux at the water-air interface versus salinity (Figure 5c) [*Udovičić et al.*, 2007]. Supersaturated porewater methane concentrations were observed at sites from the inner zone to the outer zone of Celestún Lagoon and did not show any correlation with the salinity of the overlying water. Additionally, high surface water methane concentrations and fluxes were observed at sites with high salinities in both Chelem Lagoon (harbor site) and Terminos Lagoon (canal sites). The high surface water methane concentrations measured in these three lagoons appear to be controlled by the very high porewater methane concentrations in the sediments throughout the lagoons with little relation to salinity. Methane is released from the sediments through both diffusion and ebullition, and it appears that the rates of aerobic and anaerobic methane oxidation within the lagoon sediments were insufficient to counter benthic methane production and significantly reduce methane transport to the surface waters [*Chuang et al.*, 2016]. In both Chelem and Terminos Lagoons, areas with direct pollution inputs had much higher methane concentrations than areas farther away from pollution

sources. It is possible that sewage and other wastewater inputs supply reactive organic substrates to the sediments which can be used as electron donors by methanogens, further increasing methane production rates and fluxes from the sediment to the water column [*Holmer and Kristensen*, 1994; *Oremland and Polcin*, 1982, *Chuang et al.*, 2016].

7.2. Surface Water Methane Emissions

Fluxes obtained during this study greatly expand the number of published methane fluxes from tropical lagoon systems in the Americas, and they also represent a wide range of environmental conditions and levels of anthropogenic impacts. The diffusive flux calculated for the canals in Terminos was higher than any of the previously reported total methane fluxes for mangrove-surrounded systems in the Americas [*Barber et al.*, 1988; *Sotomayor et al.*, 1994]. Additionally, average diffusive fluxes from Celestún, a relatively pristine system, were generally much higher than the fluxes reported by *Harriss et al.* [1988] and *Sotomayor et al.* [1994] for moderate- to high-salinity, nonpolluted mangrove-surrounded areas in Florida and Puerto Rico. The highest diffusive flux measured in Celestún (15 mmol CH_4 m^{-2} d^{-1}) was in the higher range of the fluxes reported for relatively undisturbed moderate to high-salinity mangrove-surrounded systems and associated water bodies in India (4.6 to 11 mmol CH_4 m^{-2} d^{-1}) [*Purvaja and Ramesh*, 2001; *Verma et al.*, 1999]. Our flux chamber measurements fell within the range of total methane flux reported for the Indian mangrove-surrounded lagoon systems, and two of our sites, 1CHa and 2TER, showed higher total methane fluxes than any of the reported values for any mangrove-surrounded systems. While the majority of chamber flux measurements were lower than average bubble fluxes reported for freshwater and coastal environments, the total fluxes measured at 1CHa and 2TER were higher than those reported for freshwater systems [*Bartlett et al.*, 1988, 1990; *Chanton et al.*, 1989; *Hirota et al.*, 2007; *Keller and Stallard*, 1994; *Miller and Oremland*, 1988; *Verma et al.*, 2002; *Ferrón et al.*, 2007; *Deborde et al.*, 2010].

All of the chambers that recorded higher fluxes than the calculated diffusive fluxes showed distinct nonlinear increases in methane concentration, which in several instances coincided with direct observation of bubbles entering the chambers [*Keller and Stallard*, 1994; *Miller and Oremland*, 1988]. It appears that ebullition is prevalent in these sites, and this is also supported by our observations of bubbles throughout the lagoons particularly at low tide.

Another observation that is consistent with the prominence of ebullition is the higher diffusive methane emissions from water to air than the total dissolved methane flux from the sediment to the water column at many sites (Figure 4 and Tables S1 and S2). Since the only methane source to the shallow oxic water column in these lagoons is the sediments [*Chuang et al.*, 2016], the implication is that additional methane is entering the water column from the sediments through bubble ebullition. Ebullition will occur when gas bubbles form when/where porewater methane concentrations are higher than the saturation concentration and the buoyancy of the gas bubbles exceeds the mechanical retardation of the sediment. Since gas transport from the sediment to the overlying water is rapid with minimal interaction with the pore fluid [*Martens et al.*, 1998], AOM is insufficient to prevent methane from escaping to the bottom water [*Chuang et al.*, 2016]. Aerobic methane oxidation in these shallow well-oxygenated water columns is also insufficient to prevent methane from reaching the atmosphere. Overall, the combined diffusive and ebullition fluxes reported here suggest a considerable source of methane to the atmosphere from the sediments. The atmospheric methane fluxes based on diffusive transport are minimum estimates. The bubble flux is likely to be a very important and under studied component of methane flux from mangrove-surrounded lagoon and coastal systems. Due to the sporadic nature of ebullition, additional more systematic studies are needed to more accurately estimate the contribution of bubble flux to the total atmospheric methane flux from mangrove-surrounded water systems. Our data set, albeit limited, indicates that the ebullition associated flux of methane to the atmosphere at our sites and likely at similar settings in other mangrove-surrounded water bodies could be 2 orders of magnitude higher than the diffusive flux.

7.3. Tidal Variations

The results of the tidal/diurnal cycle sampling in Celestún Lagoon show that there is considerable short-term variability in surface water methane concentrations even at single locations. The maximum in surface water methane concentrations at all three stations occurred in the early hours of the day, typically coinciding with low tide (Figure 3). Much greater variability in methane concentrations was observed near the sides of the

lagoon compared to the center, possibly due to the greater depth in the center where an artificial boat channel has been excavated. These results also indicate that surface water methane concentrations measured along the sides of the lagoon are more sensitive to tides than those in the center of the lagoon. *Chanton et al.* [1989] found that decreases in hydrostatic pressure caused by low tide led to increases in methane bubble flux from underlying sediments. Since tidal changes will result in a larger relative change in water column depth along the sides of the lagoon (<1 m depth and 0.5 m tidal ranges) than in the center of the lagoon (~1.75 m depth), methane concentrations in the water column may be more tidally influenced along the sides. The large increase in methane concentrations in the water column during low tide indicates that the tides affect methane release from the sediments by modulating the pressure and hence gas solubility in pore waters [*Scandella et al.*, 2011, *Middelburg et al.*, 1996]. Tidally mediated exchange of porewater between sediments and surface waters has been recognized previously [*Bouillon et al.*, 2007a, 2007b; *Dittmar and Lara*, 2001; *Gleeson et al.*, 2013; *Li et al.*, 2009; *Maher et al.*, 2013; *Robinson et al.*, 2007; *Santos et al.*, 2012].

Applying the maximum change of tidal height in this study (Figure 3) for core 6CEL_Jul02, methane solubility should decrease by about 0.05 mM at low tide [*Duan et al.*, 1992]. This solubility change is equal to an increase in the free gas content of 8.4 mmol m^{-2} over 6 h (~1/2 tidal cycle) if pore waters are oversaturated, calculated assuming an average porosity of 0.84 and a sediment length of 20 cm. This is comparable to a mean chamber flux of 46.5 mmol CH_4 m^{-2} d^{-1} in this lagoon, implying that tidal variations may account for a significant fraction of the fluxes we calculated based on the flux chamber measurements. Notably, these values are an order of magnitude higher than the model-derived methane flux at the sediment-water interface (2.5 mmol CH_4 m^{-2} d^{-1}), which also highlights the importance of direct escape of methane from the sediment as gas bubbles [*Chuang et al.*, 2016]. Indeed, measured porewater methane concentrations were oversaturated for core 6CEL_Jul02, consistent with gas formation and ebullition. This also implies that the entire lagoon might be affected by tidally driven gas release since methane oversaturation in porewaters was observed throughout Celestún Lagoon, e.g., sites 2CEL, 3CEL, 6CEL, 8CEL, 11CEL, 13CEL, and 14CEL (Figure S1 in the supporting information). Ebullition is not easy to quantify accurately [*Lindgren et al.*, 2016, and references therein], and our samples were not collected using a statistically rigorous sampling methodology, but they serve to illustrate the prevalence of ebullition and emphasize the importance of obtaining better estimates of these fluxes from mangrove-dominated lagoons around the world.

7.4. Mangrove-Surrounded Water Bodies Contribution to the Global Methane Budget

The data from this study and several studies from India suggest that the atmospheric methane contribution from mangrove-surrounded water bodies is considerable and is likely to increase due to pollution inputs. Estimating the methane contribution of mangrove-surrounded water bodies to the global methane budget involves large uncertainties, particularly because few measurements are available for mangrove-surrounded water bodies in comparison to other wetland types. In addition, there is not a single report that provides a robust estimate of the ebullition fluxes from such systems due to the sporadic nature of such fluxes and the extensive effort associated with designing and implementing statistically rigorous sampling methodology and collecting data globally based on the established sampling protocol. Another major uncertainty rests with the global surface area of the mangrove-surrounded water bodies. In an earlier study, the ratio of total world mangrove forest covered area (171,000 km^2) to the total mangrove-associated open-water surface area (lagoons and estuaries) (82,535.3 km^2) was estimated to be approximately 2 [*Caddy and Sharp*, 1986]. This ratio falls in the range of ratios (2 to 10) given by *Alongi* [2009] for mangrove forest area to waterway area in some mangrove ecosystems. However, the total coastal lagoon covered area in Mexico (15,673 km^2) [*Contreras-Espinosa and Warner*, 2004]) is larger than the mangrove forests covered (7738 km^2) [*Valderrama et al.*, 2014]), giving a ratio of 0.49 (forest to lagoon). This is not unique, for example, the Andaman Islands [*Linto et al.*, 2014] are characterized by an even lower ratio of 0.33 (water bodies = 2700 km^2, total mangrove forests covered area = 892 km^2).

Despite the large uncertainty that would be involved in extrapolating the data from our samples regionally and let alone globally an "order of magnitude" calculation would be useful for demonstrating the potential importance (or lack of) of these systems in the global methane budget. If we assume that the seasonally weighted average diffusive flux from Celestún (1.9 mmol CH_4 m^{-2} d^{-1}) is representative of pristine

mangrove-surrounded water bodies in Mexico [*Contreras-Espinosa and Warner*, 2004]), then the total diffusive annual lagoon water atmospheric emissions in Mexico amount to 0.17 Tg CH_4 yr^{-1}. If these emission rates are similar to the global average emission rates then upscaling this to the mangrove-surrounded water bodies worldwide (69,000 km^2; determined by using a ratio of 2 for the current estimated total world mangrove surface area of 138,000 km^2 [*Giri et al.*, 2011]) implies that mangrove-surrounded water bodies could account for up to 0.43% of the most recent global methane flux estimate from wetlands (177 to 284 Tg CH_4 yr^{-1} [*Kirschke et al.*, 2013]). However, all data suggest that actual fluxes from these systems are much higher due to the prevalence of ebullition which is hard to precisely quantify. In Celestún, total methane flux measured in each chamber was up to 100 times greater than the diffusive flux and on average 10 times greater than the calculated diffusive flux for an individual station. A conservative calculation using the average measured chamber flux (46.5 mmol CH_4 m^{-2} d^{-1}) in Celestún Lagoon to represent the atmospheric methane flux from mangrove-associated water bodies worldwide, mangrove waters could account for between 7 and 11% of the total wetland flux to the atmosphere. We realize that this calculation is based on limited data from only 3 lagoons in Mexico, but this emphasizes the potential importance of this source and the need for further more focused studies. Specifically, results of our study and previous research conducted in moderate- to high-salinity mangrove-surrounded systems of India [e.g., *Dutta et al.*, 2015] support the assertion that these systems may be important contributors to the total global methane flux from wetlands.

Methane fluxes from polluted mangrove-surrounded lagoon areas indicate that these areas are even larger methane sources in comparison to undisturbed systems, and with increasing development in coastal areas with mangroves this may be even more prevalent in the future. Based on average measured surface water concentrations and an average seasonal wind speed, the calculated average diffusive methane flux from the polluted Terminos canal was 7.7 mmol CH_4 m^{-2} d^{-1}, and in India average annual emissions range from 7.5 to 59 mmol CH_4 m^{-2} d^{-1} for polluted areas [*Biswas et al.*, 2004, 2007; *Purvaja and Ramesh*, 2001; *Verma et al.*, 1999, 2002; *Dutta et al.*, 2015]. Total fluxes (diffusion and ebullition) for the polluted areas were 10 to 100 times higher than for the pristine areas. Hence, with many mangrove-surrounded water bodies worldwide impacted by pollution [*Ramesh et al.*, 2007; *Purvaja and Ramesh*, 2001; *Sotomayor et al.*, 1994; *Giani et al.*, 1996; *Kreuzwieser et al.*, 2003; *Chen et al.*, 2010, 2011] our estimate based on the fluxes from pristine settings is likely to underestimate the true importance of these system to the global methane budget. Moreover, with increasing development along mangrove dominated coastlines and use of these systems for aquaculture and other activities, methane fluxes from these systems are likely to increase in the future.

Finally, it is worth noting that geological evidence and modern observations suggest that the extent of mangrove-surrounded systems can respond rapidly to climate change, particularly to changes in sea level [*Field*, 1995; *Ellison and Stoddart*, 1991; *Krauss et al.*, 2014; *Mckee et al.*, 2007; *Semeniuk*, 1994]. Past expansion of mangrove-surrounded areas during interglacials may have resulted in increased methane emissions from coastal areas and should be considered in paleo-reconstructions and future projections of atmospheric methane budgets.

8. Summary

Methane dynamics from mangrove-surrounded tropical coastal lagoons in Yucatán, Mexico, are controlled by multiple processes, including physical processes such as mixing with seawater or groundwater and tidal pumping and biological processes such as sulfate reduction and methane production and oxidation. These multiple sources and sinks result in significant temporal and spatial variations in methane concentrations and fluxes from mangrove-surrounded lagoons. Despite high salinity and high sulfate concentrations, methane production rates in the Yucatán mangrove sediments are high and methane accumulates in porewaters at shallow depths due to high organic matter content in the sediment and the use of noncompetitive substrates by methanogenic microorganisms [*Chuang et al.*, 2016]. This, combined with the shallow water depth of the lagoons and tidally modulated changes in pressure, results in high methane fluxes from the sediment to the water column and from the water column to the atmosphere. If fluxes from these sites are representative of other mangrove associated water bodies, fluxes from these systems can potentially account for a substantial fraction of the total global wetland flux to the atmosphere. Our results also

indicate that pollution increases methane fluxes by 10–100 folds, and taking this into account may increase the global contribution from these systems considerably.

Mangrove-surrounded systems throughout the world are facing rapidly increasing modification such as destruction and pollution from development. Although mangroves only account for a small fraction of the total wetlands and estuarine areas, the results of this study suggest that mangrove-surrounded water bodies, particularly those with pollution inputs, can produce much higher atmospheric methane fluxes than other types of moderate- to high-salinity coastal and estuarine areas, with fluxes similar to freshwater systems. This is an important consideration for past and future atmospheric methane budgets.

Acknowledgments
We thank the staff of the DUMAC Celestún station, the students of CINVESTAV, and the staff of the Universidad Nacional Autónoma de México (UNAM) Terminos field station for their assistance with laboratory space, lodging, and field work. We thank Tom Lorenson and Ron Oremland of the Menlo Park, CA, USGS for facility use and analyses. Meagan Eagle Gonneea, Derek Fong, and Eitan Popper and the Paytan laboratory members provided invaluable assistance with sample collection, instrument deployment, and data interpretation. This work was funded by US National Science Foundation award INT 009214214 to A.P., Consejo Nacional de Ciencia y Tecnología ref: 4147-P T9608, 32356T, and CONABIO ref: B019 to J.H.-S., a Stanford Graduate Fellowship to M.Y. and P.C.C. funded through DFG-Research Center/Cluster of Excellence "The Ocean in the Earth System"(Sediment Geochemistry).

References

Alongi, D. M. (2009), *The Energetics of Mangrove Forests*, p. 216, Springer Press, London.
Barber, T. R., R. A. Burke, and W. M. Sackett (1988), Diffusive flux of methane from warm wetlands, *Global Biogeochem. Cycles*, *2*, 411–425.
Barbier, E. B., and I. Strand (1998), Valuing mangrove-fishery linkages, *Environ. Resour. Econ.*, *12*, 151, doi:10.1023/A:1008248003520.
Barnes, R. O., and E. D. Goldberg (1976), Methane production and consumption in anoxic marine sediments, *Geology*, *4*(5), 297–300, doi:10.1130/0091-7613(1976)4<297:mpacia>2.0.co;2.
Bartlett, K. B., R. C. Harriss, and D. I. Sebacher (1985), Methane flux from coastal salt marshes, *J. Geophys. Res.*, *90*, 5710–5720.
Bartlett, K. B., D. S. Bartlett, R. C. Harriss, and D. I. Sebacher (1987), Methane emissions along a salt marsh salinity gradient, *Biogeochemistry*, *4*(3), 183–202.
Bartlett, K. B., P. M. Crill, D. I. Sebacher, R. C. Harriss, J. O. Wilson, and J. M. Melack (1988), Methane flux from the central Amazonian floodplain, *J. Geophys. Res.*, *93*, 1571–1582.
Bartlett, K. B., P. M. Crill, J. A. Bonassi, J. E. Richey, and R. C. Harriss (1990), Methane flux from the Amazon River floodplain: Emissions during rising water, *J. Geophys. Res.*, *95*, 16,773–16,788.
Bastviken, D., J. Cole, M. Pace, and L. Tranvik (2004), Methane emissions from lakes: Dependence of lake characteristics, two regional assessments, and a global estimate, *Global Biogeochem. Cycles*, *18*, GB4009, doi:10.1029/2004GB002238.
Berner, R. A. (1980), *Early Diagenesis. A Theoretical Approach*, p. 241, Princeton Univ. Press, Princeton, N. J.
Bergamaschi, B. A., D. P. Krabbenhoft, G. R. Aiken, E. Patino, D. G. Rumbold, and W. H. Orem (2012), Tidally driven export of dissolved organic carbon, total mercury, and methyl mercury from a mangrove-dominated estuary, *Environ. Sci. Technol.*, *46*(3), 1371–1378.
Biswas, H., S. K. Mukhopadhyay, T. K. De, S. Sen, and T. K. Jana (2004), Biogenic controls on the air—Water carbon dioxide exchange in the Sundarban mangrove environment, northeast coast of bay of Bengal, India, *Limnol. Oceanogr.*, *49*(1), 95–101.
Biswas, H., S. K. Mukhopadhyay, S. Sen, and T. K. Jana (2007), Spatial and temporal patterns of methane dynamics in the tropical mangrove dominated estuary, NE coast of Bay of Bengal, India, *J. Mar. Syst.*, *68*(1–2), 55–64.
Boudreau, B. P. (1997), *Diagenetic Models and Their Implementation: Modelling Transport and Reactions in Aquatic Sediments*, pp. 6–21, Springer, Berlin.
Bouillon, S., F. Dehairs, L.-S. Schiettecatte, and A. V. Borges (2007a), Biogeochemistry of the Tana estuary and delta (northern Kenya), *Limnol. Oceanogr.*, *52*(1), 46–59.
Bouillon, S., J. J. Middelburg, F. Dehairs, A. V. Borges, G. Abril, M. R. Flindt, S. Ulomi, and E. Kristensen (2007b), Importance of intertidal sediment processes and porewater exchange on the water column biogeochemistry in a pristine mangrove creek (Ras Dege, Tanzania), *Biogeosciences*, *4*(3), 311–322.
Bouillon, S., et al. (2008), Mangrove production and carbon sinks: A revision of global budget estimates, *Global Biogeochem. Cycles*, *22*, GB2013, doi:10.1029/2007GB003052.
Caddy, J. F., and G. D. Sharp (1986), An ecological framework for marine fishery investigations. *FAO Fish. Tech. Pap.* No. 283, 152pp.
Call, M., et al. (2015), Spatial and temporal variability of carbon dioxide and methane fluxes over semi-diurnal and spring–neap–spring timescales in a mangrove creek, *Geochim. Cosmochim. Acta*, *150*, 211–225.
Chanton, J. P., C. S. Martens, and C. A. Kelley (1989), Gas transport from methane-saturated, tidal freshwater and wetland sediments, *Limnol. Oceanogr.*, *34*(5), 807–819.
Chen, G. C., N. F. Y. Tam, and Y. Ye (2010), Summer fluxes of atmospheric greenhouse gases N_2O, CH_4 and CO_2 from mangrove soil in South China, *Sci. Total Environ.*, *408*(13), 2761–2767, doi:10.1016/j.scitotenv.2010.03.007.
Chen, G. C., N. F. Y. Tam, Y. S. Wong, and Y. Ye (2011), Effect of wastewater discharge on greenhouse gas fluxes from mangrove soils, *Atmos. Environ.*, *45*(5), 1110–1115, doi:10.1016/j.atmosenv.2010.11.034.
Chuang, P. C., M. B. Young, A. W. Dale, L. G. Miller, J. A. Herrera-Silveira, and A. Paytan (2016), Methane and sulfate dynamics in sediments from mangrove-dominated tropical coastal lagoons, Yucatán, Mexico, *Biogeosciences*, *13*(10), 2981–3001.
Contreras-Espinosa, F., and B. G. Warner (2004), Ecosystem characteristics and management considerations for coastal wetlands in Mexico, *Hydrobiologia*, *511*(1), 233–245, doi:10.1023/b:hydr.0000014097.74263.54.
Day, J. W., R. H. Day, M. T. Barreiro, F. Ley-Lou, and C. J. Madden (1982), Primary production in the Laguna de Terminos, a tropical estuary in the southern Gulf of Mexico, *Oceanol. Acta*, 269–276.
Day, J. W., C. Coronado-Molina, F. R. Vera-Herrera, R. Twilley, V. H. Rivera-Monroy, H. Alvarez-Guillen, R. Day, and W. Conner (1996), A 7 year record of above-ground net primary production in a southeastern Mexican mangrove forest, *Aquat. Bot.*, *55*(1), 39–60.
Deborde, J., P. Anschutz, F. Guérin, D. Poirier, D. Marty, G. Boucher, G. Thouzeau, M. Canton, and G. Abril (2010), Methane sources, sinks and fluxes in a temperate tidal lagoon: The Arcachon lagoon (SW France), *Estuarine Coastal Shelf Sci.*, *89*(4), 256–266.
Devol, A. H., J. E. Richey, B. R. Forsberg, and L. A. Martinelli (1990), Seasonal dynamics in methane emissions from the Amazon River floodplain to the troposphere, *J. Geophys. Res.*, *95*, 16,417–16,426.
Dittmar, T., and R. J. Lara (2001), Driving forces behind nutrient and organic matter dynamics in a mangrove tidal creek in North Brazil, *Estuarine Coastal Shelf Sci.*, *52*(2), 249–259.
Dittmar, T., N. Hertkorn, G. Kattner, and R. J. Lara (2006), Mangroves, a major source of dissolved organic carbon to the oceans, *Global Biogeochem. Cycles*, *20*, GB1012, doi:10.1029/2005GB002570.
Duan, Z., N. Møller, J. Greenberg, and J. H. Weare (1992), The prediction of methane solubility in natural waters to high ionic strength from 0 to 250°C and from 0 to 1600 bar, *Geochim. Cosmochim. Acta*, *56*(4), 1451–1460.

Duarte, C. M., J. J. Middelburg, and N. Caraco (2005), Major role of marine vegetation on the oceanic carbon cycle, *Biogeosciences*, *2*(1), 1–8.
Dutta, M. K., R. Mukherjee, T. K. Jana, and S. K. Mukhopadhyay (2015), Biogeochemical dynamics of exogenous methane in an estuary associated to a mangrove biosphere: The Sundarbans, NE coast of India, *Mar. Chem.*, *170*, 1–10.
Eagle, M. (2002), Tracing organic matter sources in mangrove estuaries utilizing $\delta^{13}C$, $\delta^{15}N$ and C/N ratios, Master Thesis, Stanford Univ., Stanford, Calif.
Ellison, J. C., and D. R. Stoddart (1991), Mangrove ecosystem collapse during predicted sea-level rise: Holocene analogues and implications, *J. Coast. Res.*, *7*(1), 151–165.
Ezcurra, P., E. Ezcurra, P. P. Garcillán, M. T. Costa, and O. Aburto-Oropeza (2016), Coastal landforms and accumulation of mangrove peat increase carbon sequestration and storage, *Proc. Natl. Acad. Sci.*, *113*(16), 4404–4409.
Ferrón, S., T. Ortega, A. Gómez-Parra, and J. M. Forja (2007), Seasonal study of dissolved CH_4, CO_2 and N_2O in a shallow tidal system of the bay of Cádiz (SW Spain), *J. Mar. Syst.*, *66*(1–4), 244–257, doi:10.1016/j.jmarsys.2006.03.021.
Field, C. D. (1995), Impact of expected climate change on mangroves, *Hydrobiologia*, *295*(1), 75–81.
Food and Agriculture Organization Forestry (2010), Global forest resources assessment. Food and Agriculture Organization of the United Nations, Rome, Italy.
Fung, I., J. John, J. Lerner, E. Matthews, M. Prather, L. P. Steele, and P. J. Fraser (1991), Three-dimensional model synthesis of the global methane cycle, *J. Geophys. Res.*, *96*, 13,033–13,065.
Giani, L., Y. Bashan, G. Holguin, and A. Strangmann (1996), Characteristics and methanogenesis of the Balandra lagoon mangrove soils, Baja California Sur, Mexico, *Geoderma*, *72*(1), 149–160, doi:10.1016/0016-7061(96)00023-7.
Giri, C., E. Ochieng, L. L. Tieszen, Z. Zhu, A. Singh, T. Loveland, J. Masek, and N. Duke (2011), Status and distribution of mangrove forests of the world using Earth observation satellite data, *Global Ecol. Biogeogr.*, *20*(1), 154–159.
Gleeson, J., I. R. Santos, D. T. Maher, and L. Golsby-Smith (2013), Groundwater–surface water exchange in a mangrove tidal creek: Evidence from natural geochemical tracers and implications for nutrient budgets, *Mar. Chem.*, *156*, 27–37.
Gonneea, M. E., A. Paytan, and J. A. Herrera-Silveira (2004), Tracing organic matter sources and carbon burial in mangrove sediments over the past 160 years, *Estuarine Coastal Shelf Sci.*, *61*(2), 211–227.
Harriss, R. C., D. I. Sebacher, K. B. Bartlett, D. S. Bartlett, and P. M. Crill (1988), Sources of atmospheric methane in the south Florida environment, *Global Biogeochem. Cycles*, *2*, 231–243.
Herrera-Silveira, J. (1994), Nutrients from underground discharges in a coastal lagoon (Celestún, Yucatán, Mexico), *Verh. Internat. Verein. Limnol.*, *25*, 1398–1403.
Herrera-Silveira, J. A., and F. A. Comín (2000), An Introductory account of the types of aquatic ecosystems of Yucatan Peninsula (SE Mexico), in *Aquatic Ecosystems of Mexico: Status & Scope, Ecovision World Monogr. Ser.*, edited by M. Munawar et al., pp. 213–227, Backhuys Pub. Leiden, Netherlands.
Herrera-Silveira, J. A., J. R. Ramírez, and A. Zaldivar (1998), Overview and characterization of the hydrology and primary producer communities of selected coastal lagoons of Yucatán, México, *Aquat. Ecosyst. Health Manag.*, *1*(3–4), 353–372.
Herrera-Silveira, J. A., J. R. Ramírez, N. Gomez, and A. Zaldivar (2000), Seagrass bed recovery after hydrological restoration in a coastal lagoon with groundwater discharges in the north of Yucatan, in *Seagrass: Monitoring Ecology, Physiology and Management. Boca Raton*, edited by S. Bortone, pp. 123–135, CRC Press, Boca Raton, Fla.
Hirota, M., Y. Senga, Y. Seike, S. Nohara, and H. Kunii (2007), Fluxes of carbon dioxide, methane and nitrous oxide in two contrastive fringing zones of coastal lagoon, Lake Nakaumi, Japan, *Chemosphere*, *68*(3), 597–603.
Holmer, M., and E. Kristensen (1994), Coexistence of sulfate reduction and methane production in an organic-rich sediment, *Mar. Ecol. Prog. Ser.*, *107*, 177–184.
Jähne, B., G. Heinz, and W. Dietrich (1987), Measurement of the diffusion coefficients of sparingly soluble gases in water, *J. Geophys. Res.*, *92*, 10,767–10,776.
Keller, M., and R. F. Stallard (1994), Methane emission by bubbling from Gatun Lake, Panama, *J. Geophys. Res.*, *99*, 8307–8319.
Kirschke, S., et al. (2013), Three decades of global methane sources and sinks, *Nat. Geosci.*, *6*(10), 813–823, doi:10.1038/ngeo1955.
Kjerfve, B. (1981), Tides of the Caribbean Sea, *J. Geophys. Res.*, *86*, 4243–4247.
Krauss, K. W., K. L. McKee, C. E. Lovelock, D. R. Cahoon, N. Saintilan, R. Reef, and L. Chen (2014), How mangrove forests adjust to rising sea level, *New Phytol.*, *202*(1), 19–34.
Kreuzwieser, J., J. Buchholz, and H. Rennenberg (2003), Emission of methane and nitrous oxide by Australian mangrove ecosystems, *Plant Biol.*, *5*(4), 423–431.
Kristensen, E., S. Bouillon, T. Dittmar, and C. Marchand (2008a), Organic carbon dynamics in mangrove ecosystems: A review, *Aquat. Bot.*, *89*(2), 201–219.
Kristensen, E., M. R. Flindt, S. Ulomi, A. V. Borges, G. Abril, and S. Bouillon (2008b), Emission of CO_2 and CH_4 to the atmosphere by sediments and open waters in two Tanzanian mangrove forests, *Mar. Ecol. Prog. Ser.*, *370*, 53–67.
Lankford R. E. (1977), Coastal lagoons of Mexico, their origin and classification, in *Estuarine Processes*, 2, pp. 182–252, Academic Press, New York.
Li, X., B. X. Hu, W. C. Burnett, I. R. Santos, and J. P. Chanton (2009), Submarine ground water discharge driven by tidal pumping in a heterogeneous aquifer, *Ground Water*, *47*(4), 558–568.
Lindgren, P. R., G. Grosse, K. W. Anthony, and F. J. Meyer (2016), Detection and spatiotemporal analysis of methane ebullition on thermokarst lake ice using high-resolution optical aerial imagery, *Biogeosciences*, *13*(1), 27.
Linto, N., J. Barnes, R. Ramachandran, J. Divia, P. Ramachandran, and R. C. Upstill-Goddard (2014), Carbon dioxide and methane emissions from mangrove-associated waters of the Andaman Islands, Bay of Bengal, *Estuaries Coasts*, *37*(2), 381–398.
Liss, P. S., and P. G. Slater (1974), Flux of gases across the air-sea interface, *Nature*, *247*(5438), 181–184.
Liss, P. S., L. Merlivat (1986), Air-sea gas exchange rates: Introduction and synthesis, in *The Role of Air-Sea Exchange in Geochemical Cycling*, edited by P. Buat-Menard, pp. 112–127, D. Reidel, Dordrecht, Netherlands.
Maher, D. T., I. R. Santos, L. Golsby-Smith, J. Gleeson, and B. D. Eyre (2013), Groundwater-derived dissolved inorganic and organic carbon exports from a mangrove tidal creek: The missing mangrove carbon sink?, *Limnol. Oceanogr.*, *58*(2), 475–488.
Marchand, C., P. Albéric, E. Lallier-Vergès, and F. Baltzer (2006), Distribution and characteristics of dissolved organic matter in mangrove sediment pore waters along the coastline of French Guiana, *Biogeochemistry*, *81*(1), 59–75.
Martens, C. S., D. B. Albert, and M. J. Alperin (1998), Biogeochemical processes controlling methane in gassy coastal sediments—Part 1. A model coupling organic matter flux to gas production, oxidation and transport, *Cont. Shelf Res.*, *18*(14), 1741–1770.
Matthews, E., and I. Fung (1987), Methane emission from natural wetlands: Global distribution, area, and environmental characteristics of sources, *Global Biogeochem. Cycles*, *1*, 61–86.

McKee, K. L., D. R. Cahoon, and I. C. Feller (2007), Caribbean mangroves adjust to rising sea level through biotic controls on change in soil elevation, *Global Ecol. Biogeogr.*, *16*(5), 545–556.
Medina-Gómez, I., G. J. Villalobos-Zapata, and J. A. Herrera-Silveira (2015), Spatial and temporal hydrological variations in the inner estuaries of a large coastal lagoon of the southern Gulf of Mexico, *J. Coast. Res.*, *31*, 1429–1438.
Middelburg, J. J., G. Klaver, J. Nieuwenhuize, A. Wielemaker, W. de Haas, T. Vlug, and J. van der Nat (1996), Organic matter mineralization in intertidal sediments along an estuarine gradient, *Mar. Ecol. Prog. Ser.*, *132*, 157–168.
Miller, L. G., and R. S. Oremland (1988), Methane efflux from the pelagic regions of four lakes, *Global Biogeochem. Cycles*, *2*, 269–277.
Oremland, R. S., and S. Polcin (1982), Methanogenesis and sulfate reduction: Competitive and noncompetitive substrates in estuarine sediments, *Appl. Environ. Microbiol.*, *44*(6), 1270–1276.
Podgrajsek, E., E. Sahlée, D. Bastviken, J. Holst, A. Lindroth, L. Tranvik, and A. Rutgersson (2014), Comparison of floating chamber and eddy covariance measurements of lake greenhouse gas fluxes, *Biogeosciences*, *11*(15), 4225–4233.
Poffenbarger, H. J., B. A. Needelman, and J. P. Megonigal (2011), Salinity influence on methane emissions from tidal marshes, *Wetlands*, *31*(5), 831–842.
Purvaja, R., and R. Ramesh (2001), Natural and anthropogenic methane emission from coastal wetlands of South India, *Environ. Manage.*, *27*(4), 547–557.
Purvaja, R., R. Ramesh, and P. Frenzel (2004), Plant-mediated methane emission from an Indian mangrove, *Global Change Biol.*, *10*(11), 1825–1834.
Ramesh, R., R. Purvaja, V. Neetha, J. Divia, J. Barnes, R. Upstill-Goddard (2007), CO_2 and CH_4 emissions from Indian mangroves and its surrounding waters, in *Greenhouse Gas and Carbon Balances in Mangrove Coastal Ecosystems, Proceedings*, edited by Y. Tateda, pp. 153–164, Gendai Tosho, Kanagawa, Japan.
Rejmankova, E., and R. A. Post (1996), Methane in sulfate-rich and sulfate-poor wetland sediments, *Biogeochemistry*, *34*(2), 57–70, doi:10.1007/bf02180973.
Ringeval, B., S. Houweling, P. M. van Bodegom, R. Spahni, R. van Beek, F. Joos, and T. Röckmann (2014), Methane emissions from floodplains in the Amazon Basin: Challenges in developing a process-based model for global applications, *Biogeosciences*, *11*(6), 1519–1558.
Rivera-Monroy, V. H., C. J. Madden, J. W. Day, R. R. Twilley, F. Vera-Herrera, and H. Alvarez-Guillén (1998), Seasonal coupling of a tropical mangrove forest and an estuarine water column: Enhancement of aquatic primary productivity, *Hydrobiologia*, *379*(1), 41–53, doi:10.1023/a:1003281311134.
Robertson, A. I., D. M. Alongi, and K. G. Boto (2013), Food chains and carbon fluxes, in *Tropical Mangrove Ecosystems*, edited by A. I. Robertson, and D. M. Alongi, pp. 293–326, AGU, Washington, D. C.
Robinson, C., L. Li, and H. Prommer (2007), Tide-induced recirculation across the aquifer-ocean interface, *Water Resour. Res.*, *43*, W07428, doi:10.1029/2006WR005679.
Rudd, J., R. Hamilton, and N. Campbell (1974), Measurement of microbial oxidation of methane in lake water, *Limnol. Oceanogr.*, *19*(3), 519–524.
Santos, I. R., B. D. Eyre, and M. Huettel (2012), The driving forces of porewater and groundwater flow in permeable coastal sediments: A review, *Estuarine Coastal Shelf Sci.*, *98*, 1–15.
Scandella, B. P., C. Varadharajan, H. F. Hemond, C. Ruppel, and R. Juanes (2011), A conduit dilation model of methane venting from lake sediments, *Geophys. Res. Lett.*, *38*, L06408, doi:10.1029/2011GL046768.
Segarra, K. E. A., C. Comerford, J. Slaughter, and S. B. Joye (2013), Impact of electron acceptor availability on the anaerobic oxidation of methane in coastal freshwater and brackish wetland sediments, *Geochim. Cosmochim. Acta*, *115*, 15–30.
Semeniuk, V. (1994), Predicting the effect of sea-level rise on mangroves in northwestern Australia, *J. Coast. Res.*, *10*, 1050–1076.
Sotomayor, D., J. E. Corredor, and J. M. Morell (1994), Methane flux from mangrove sediments along the southwestern coast of Puerto Rico, *Estuaries*, *17*(1), 140–147.
Tapia González, F. U., J. A. Herrera-Silveira, and M. L. Aguirre-Macedo (2008), Water quality variability and eutrophic trends in karstic tropical coastal lagoons of the Yucatán Peninsula, *Estuarine Coastal Shelf Sci.*, *76*(2), 418–430, doi:10.1016/j.ecss.2007.07.025.
Tenorio-Fernandez, L., J. Gomez-Valdes, I. Marino-Tapia, C. Enriquez, A. Valle-Levinson, and S. M. Parra (2016), Tidal dynamics in a frictionally dominated tropical lagoon, *Cont. Shelf Res.*, *114*, 16–28.
Udovičić, M., K. Baždarić, L. Bilić-Zulle, and M. Petrovečki (2007), What we need to know when calculating the coefficient of correlation?, *Biochem. Med.*, *17*(1), 10–15.
Valderrama, L., C. Troche, M. T. Rodriguez, D. Marquez, B. Vázquez, S. Velázquez, A. Vázquez, M. I. Cruz, and R. Ressl (2014), Evaluation of mangrove cover changes in mexico during the 1970–2005 period, *Wetlands*, *34*(4), 747–758.
Valdes, D. S., and E. Real (1998), Variations and relationships of salinity, nutrients and suspended solids in Chelem coastal lagoon at Yucatan, Mexico, *Indian J. Mar. Sci.*, *27*, 149–156.
Verma, A., V. Subramanian, and R. Ramesh (1999), Day-time variation in methane emission from two tropical urban wetlands in Chennai, Tamil Nadu, India, *Curr. Sci.*, *76*(7), 1020–1022.
Verma, A., V. Subramanian, and R. Ramesh (2002), Methane emissions from a coastal lagoon: Vembanad Lake, West Coast, India, *Chemosphere*, *47*(8), 883–889.
Wanninkhof, R. (1992), Relationship between wind speed and gas exchange over the ocean, *J. Geophys. Res.*, *97*, 7373–7382.
Whalen, S. C. (2005), Biogeochemistry of methane exchange between natural wetlands and the atmosphere, *Environ. Eng. Sci.*, *22*(1), 73–94.
Wiesenburg, D. A., and N. L. Guinasso (1979), Equilibrium solubilities of methane, carbon monoxide, and hydrogen in water and sea water, *J. Chem. Eng. Data*, *24*(4), 356–360.
Yamamoto, S., J. B. Alcauskas, and T. E. Crozier (1976), Solubility of methane in distilled water and seawater, *J. Chem. Eng. Data*, *21*, 78–80.
Yanez-Arancibia, A., and J. Day (1982), Ecological characterization of Terminos lagoon, a tropical estuary in the southern Gulf of Mexico, *Oceanologica Acta.*, *43*, 1–440.
Young, M. B., M. E. Gonneea, D. A. Fong, W. S. Moore, J. Herrera-Silveira, and A. Paytan (2008), Characterizing sources of groundwater to a tropical coastal lagoon in a karstic area using radium isotopes and water chemistry, *Mar. Chem.*, *109*(3–4), 377–394.